Large Seebeck effect in electron-doped $FeAs_2$ driven by a quasi-one-dimensional pudding-mold-type band

Hidetomo Usui,[1,2] Katsuhiro Suzuki,[3] Kazuhiko Kuroki,[1,2] Seiya Nakano,[4,2] Kazutaka Kudo,[4,2] and Minoru Nohara[4,2]

[1]*Department of Physics, Osaka University, 1-1 Machikaneyama-cho, Toyonaka, Osaka 560-0043, Japan*

[2]*JST, ALCA, Gobancho, Chiyoda, Tokyo 102-0075, Japan*

[3]*Department of Engineering Science, The University of Electro-Communication, Chofu, Tokyo 182-8585, Japan*

[4]*Department of Physics, Okayama University, Okayama 700-8530, Japan*

(Received 30 November 2012; revised manuscript received 11 July 2013; published 26 August 2013)

We investigate the thermoelectric properties of the electron-doped $FeAs_2$ both experimentally and theoretically. Electrons are doped by partially substituting Se for As, which leads to a metallic behavior in the resistivity. A Seebeck coefficient of about $-200\ \mu V/K$ is reached at 300 K for 1% doping, and about $-120\ \mu V/K$ even at 5% doping. The origin of this large Seebeck coefficient, despite the metallic conductivity, is analyzed from a band structure point of view. The first-principles band calculation reveals the presence of a pudding-mold-type band just above the band gap, somewhat similar to Na_xCoO_2, but with a quasi-one-dimensional nature. We calculate the Seebeck coefficient using a tight-binding model that correctly reproduces this band structure, and this gives results roughly in agreement with the experiments. Moreover, a consideration of electron correlations beyond the generalized gradient approximation by the fluctuation exchange method gives even better agreement. The origin of this peculiar band shape is also discussed. Combined with previous studies, we now have good thermoelectric materials with quasi-one-, two-, and three-dimensional band structures that have partially flat portions. The present study reinforces the general efficiency of this peculiar band shape in thermoelectric materials.

DOI: 10.1103/PhysRevB.88.075140 PACS number(s): 72.15.Jf, 63.20.dk, 71.20.−b

I. INTRODUCTION

Searching materials with good thermoelectric properties has been an issue of great interest both from the viewpoint of fundamental physics and application purposes. The efficiency of a thermoelectric material is often evaluated by the dimensionless figure of merit $ZT = S^2T/(\rho\kappa)$, where S is the Seebeck coefficient, ρ the electrical resistivity, κ the thermal conductivity, and T the temperature.[1] S^2/ρ in the ZT formula is called the power factor, and in order for this quantity to be large, both a large Seebeck coefficient and small resistivity are required. However, it is usually difficult to have a large Seebeck effect in metallic materials because holes and electrons usually have nearly the same group velocity when the Fermi level lies in the middle of a band.

The discovery of the large Seebeck effect in Na_xCoO_2 (Ref. 2) has provided a new avenue for searching good thermoelectric properties in materials with metallic resistivity with a significant amount of carriers. The power factor S^2/ρ is comparable to that of Bi_2Te_3(about 40 $\mu W/cm\ K^2$).[3] In fact, such a coexistence of metallic resistivity and large Seebeck coefficient have also been observed in, e.g., $CuRhO_2$,[4,5] $LiRh_2O_4$,[6] $LaRhO_3$,[7] $SrTiO_3$,[8,9] and quite recently, in $PtSb_2$.[10] Theoretical studies on the origin of the large Seebeck effect in these materials have also been extensively performed.[11–19] In particular, Kuroki and Arita pointed out in Ref. 19 that a peculiar band shape referred to as the "pudding-mold" type, which consists of a dispersive portion and a flat portion, can in general be favorable for the coexistence of large Seebeck coefficient and small resistivity. The quasi-two-dimensional pudding-mold band has been proposed as an origin of the large power factor observed in Na_xCoO_2 and other materials. On the other hand, Mori *et al*. have recently studied the origin of the large Seebeck effect in $PtSb_2$, and found a three-dimensional "corrugated" flatband that gives rise to many Fermi surface pockets through the entire Brillouin zone when holes are doped.[12] This also gives rise to a coexisting large Seebeck coefficient and metallic resistivity in general.

In the present study, we focus on $FeAs_2$ in an attempt to look for yet another material that exhibits a large Seebeck effect despite the metallic resistivity. $FeAs_2$ crystallizes in an orthorhombic Marcasite structure with *Pnnm* space group (no. 58). The structure is characterized by the edge-sharing $FeAs_6$ octahedra, which are connected along the crystallographic c axis (z axis) to form linear chains. The nondoped semiconductor $FeAs_2$ has been investigated previously in Ref. 20 in comparison with $FeSb_2$, which exhibits a colossal thermoelectric effect.[21] A theoretical analysis has shown that the Seebeck coefficient of the nondoped $FeAs_2$ can be understood quantitatively using the band structure obtained from the first-principles calculation.[22] In the present study, we investigate the thermoelectric properties of the *electron-doped* $FeAs_2$ both experimentally and theoretically. By doping electrons by partially substituting Se for As, the resistivity exhibits a metallic behavior, but nonetheless, we observe a fairly large Seebeck coefficient at 300 K of about $-200\ \mu V/K$ at 1% doping and $-120\ \mu V/K$ even at 5% doping. We also analyze the origin of this experimental observation theoretically. It is found that the quasi-one-dimensional (q1D) version of the pudding-mold-type band is present right above the band gap and for this peculiar band shape, and this gives Seebeck coefficient values which are roughly in agreement with the experiments. Moreover, a consideration of electron correlations beyond the generalized gradient approximation (GGA) by the fluctuation exchange method gives even better agreement. We also discuss the origin of this peculiar band shape using a simplified model. With the present study, we now have examples of materials that possess one- ($FeAs_2$),

two- (Na_xCoO_2, etc.), or three-dimensional ($PtSb_2$) flatbands that give rise to the large Seebeck coefficients with the metallic resistivity. This reinforces the general efficiency of peculiar band shapes with partially flat dispersions.

II. EXPERIMENT

A. Synthesis

Polycrystalline samples of $Fe(As_{1-x}Se_x)_2$ with nominal Se contents of $x = 0.0$, 0.01, 0.025, and 0.05 were synthesized by a solid-state reaction in two steps. First, stoichiometric amounts of starting materials Fe (99.9%), As (99.9999%), and Se (99.9%) were mixed and ground. They were heated in an evacuated quartz tube at 500°C for 40 h and then at 700°C for 40 h. Second, the product was powdered, pressed into pellets, and sintered at 800°C for 12 h. The obtained samples were characterized by powder x-ray diffraction (XRD) and confirmed to be a single phase of $Fe(As_{1-x}Se_x)_2$. The lattice parameters were changed linearly with selenium content x, suggesting the formation of solid solutions. Electrical resistivity ρ, Seebeck coefficient S, and Hall coefficient R_H were measured using a physical property measurement system (PPMS, Quantum Design) in the temperature range from 2 to 300 K.

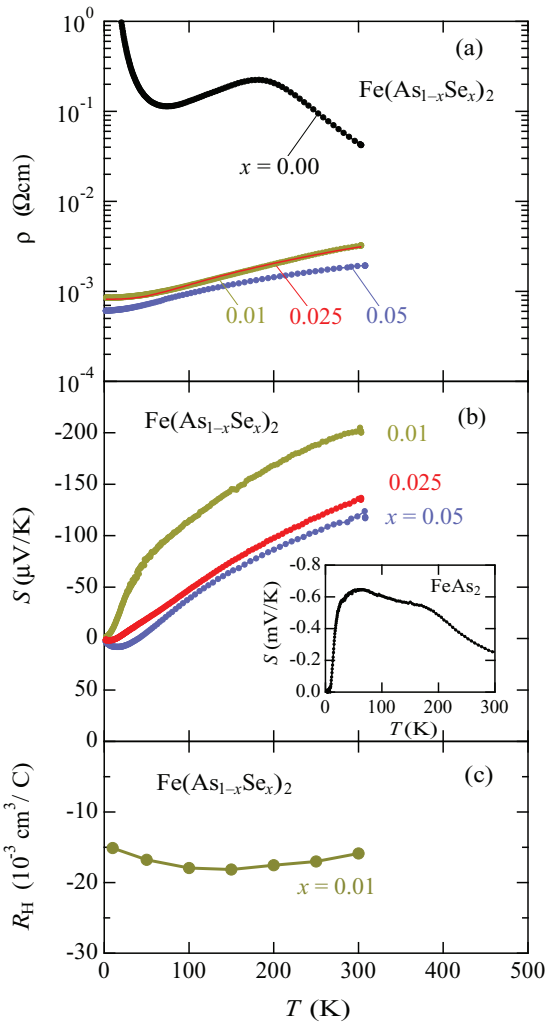

FIG. 1. (Color online) Temperature dependence of (a) electrical resistivity $\rho(T)$, (b) Seebeck coefficient $S(T)$, and (c) Hall coefficient $R_H(T)$ of polycrystalline $Fe(As_{1-x}Se_x)_2$ with $x = 0.00$, 0.01, 0.025, and 0.05. The inset shows the Seebeck coefficient of nondoped $FeAs_2$.

B. Thermoelectric properties

As shown in Fig. 1(a), nondoped $FeAs_2$ exhibits a semiconducting behavior, consistent with the previous reports.[20] The Seebeck coefficient S of the nondoped $FeAs_2$ exhibits a large maximum value of -0.65 mV/K at approximately 60 K, as shown in the inset of Fig. 1(b), which is similar to the literature data.[20] Then both the magnitude and temperature dependence of resistivity ρ changed abruptly by substituting Se for As from semiconducting to metallic. The ρ values on the order of 1 mΩ cm and the positive temperature slope of ρ suggest that a metallic state is realized for $Fe(As_{1-x}Se_x)_2$ ($x = 0.01$, 0.025, and 0.05). The temperature dependence of S is also changed abruptly by Se doping. But even in the metallic state, the Seebeck coefficient reaches a fairly large value of about -200 μV/K at 300 K for the $x = 0.01$ sample, as shown in Fig. 1(b). In this way, metallic ρ is compatible with a large S for $Fe(As_{1-x}Se_x)_2$. This combination of the resistivity and the Seebeck coefficient gives a maximum power factor of 14 $\mu W/cm\,K^2$ at approximately 200 K for the $x = 0.01$ sample.

Figure 1(c) shows the Hall coefficient R_H for the $x = 0.01$ sample as a function of temperature T. R_H is almost T independent, characteristic of metals. We estimate a carrier concentration of $n = 3.9 \times 10^{20}$ cm^{-3} at 300 K for $x = 0.01$. This value is almost comparable with a nominal value of 2×10^{20} cm^{-3} for $x = 0.01$, suggesting that Se donates one electron.

III. THEORETICAL ANALYSIS

A. Band structure

We now turn to the theoretical analysis. We perform a first-principles band structure calculation using the WIEN2K package.[23] The structural parameters adopted are given in Ref. 24, in which the lattice constants are $a = 5.268\,4$, $b = 5.963\,1$, and $c = 2.900\,7$ Å, the space group is $Pnnm$, and the atomic positions are (0,0,0) for Fe and (0.176 0,0.362 5,0) for As. In the present study, we construct tight-binding models in order to calculate the Seebeck coefficient. To obtain a model that correctly reproduces the first-principles band structure, we construct maximally localized Wannier functions (MLWFs) from the first-principles calculation result.[25] We focus on the electron-doped case up to about the room temperature, so that we only have to consider the band structure above the band gap. The tight-binding Hamiltonian is written as

$$H = \sum_{ij\sigma} \sum_{\mu\nu} t_{ij}^{\mu\nu} c_{i\mu\sigma}^{\dagger} c_{j\nu\sigma}, \qquad (1)$$

where i, j denote the sites, and μ, ν the orbitals, $t_{ij}^{\mu\nu}$ is the hopping parameter obtained from MLWFs, and $c^{\dagger}, c$ are the creation-annihilation operators. Here we first consider six orbitals (three orbitals per Fe) to reproduce the bands up to about 5 eV above the Fermi energy. These orbitals have mainly $3d$ character, although they are hybridized with As $4p$.

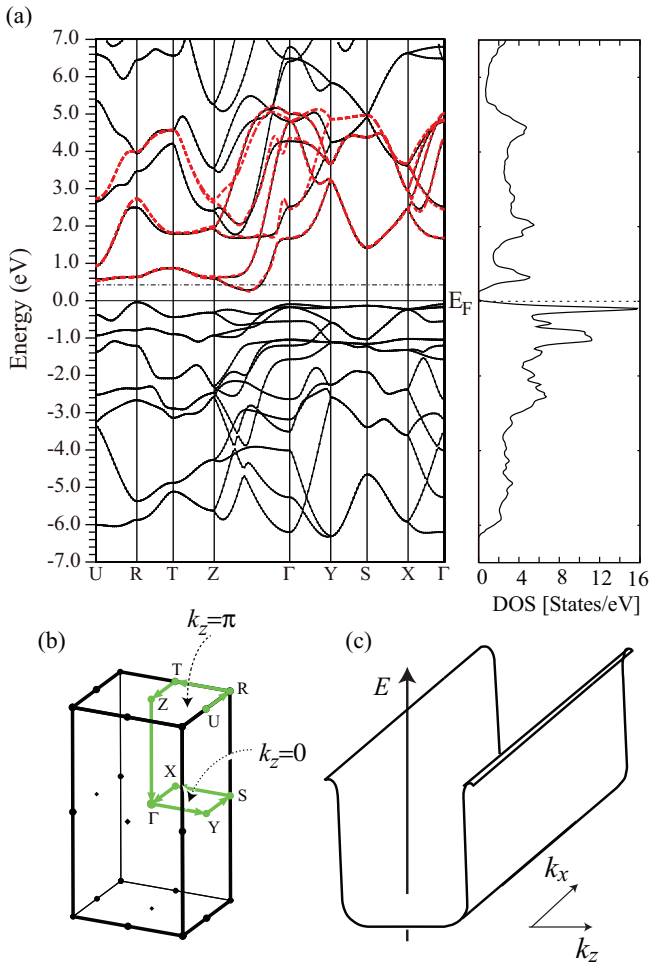

FIG. 2. (Color online) (a) The band structure and the density of states of $FeAs_2$. The solid black lines are the original first-principles band structure, while the red dashed lines are the bands of the tight-binding model constructed from MLWFs. The dash-dotted line depicts the Fermi energy for $x = 0.05$. (b) The Brillouin zone is shown. (c) A schematic image of the q1D pudding-mold-type band of $FeAs_2$.

The first-principles band structure is shown in Fig. 2(a) with the tight-binding bands superposed. The band structure just above the band gap has a nearly flat dispersion along U-R-T-Z [see (b) for the symmetrical points in the Brillouin zone], namely, within the $k_z = \pi$ plane. In fact, the Wannier orbitals that are the origin of these bands are found to be elongated in the z direction (see Fig. 6). We will call these orbitals the "d_{z^2} orbitals" for simplicity (the maximally localized Wannier orbitals are obtained by projecting onto the d_{z^2} orbital), although they are actually more complicated due to the hybridization with the As $4p$ orbitals. The quasi-one-dimensionality of the bands within the $k_z = \pi$ plane is partially because of the anisotropy of these d_{z^2} orbitals, but to be more precise, there is another factor that restricts this quasi-one-dimensionality to near the $k_z = \pi$ plane, which will be discussed later. Furthermore, these bands are somewhat flat also along Z-Γ (i.e., the k_z direction) up to some intermediate point, and then bend sharply into dispersive portions. In Fig. 2(c), we show a schematic figure of this band structure. It has a flat portion at the bottom with a q1D nature, so it is a q1D version of the pudding-mold-type band introduced in Ref. 19 as the band structure of Na_xCoO_2. This type of band structure is favorable for producing good thermoelectric properties when carriers are doped. The reason is because (i) even when a large amount of carriers are doped, the Fermi level sticks close to the band bottom due to the large density of states; (ii) for such a position of the Fermi level, there is a large difference between electron and hole group velocity [see the schematic figure in Fig. 2(c)], resulting in a large Seebeck coefficient; and (iii) small resistivity can be achieved owing to the large amount of doped carriers and the dispersive portion of the band near the Fermi level. The conductivity of the pudding-mold-type band is generally not so good as in "usual" metallic systems in which the Fermi level sits in the middle of a band and both the electrons and holes have large group velocity. The point of the theory, however, is that the conductivity is larger compared to systems with parabolic band shapes with the same position of the Fermi level (measured from the band edge), because in a parabolic band shape, the group velocity of both holes and electrons is small when the Fermi level sits close to the band edge, resulting in a large Seebeck coefficient. The origin of such a peculiar band structure in $FeAs_2$ will be discussed later.

B. Seebeck coefficient

Let us now move on to the Seebeck coefficient calculation. We first briefly introduce the method to calculate the Seebeck coefficient and the power factor.[1,14] The Seebeck coefficient S and the resistivity ρ are calculated with Boltzmann's equation using the tight-binding Hamiltonian. They are given as

$$\mathbf{S} = \frac{1}{eT}\frac{\mathbf{K}_1}{\mathbf{K}_0}, \tag{2}$$

$$\boldsymbol{\rho} = e^{-2}\mathbf{K}_0^{-1}, \tag{3}$$

where e is the elementary electrical charge ($e < 0$), and T is the temperature. $\mathbf{K}_0$ and $\mathbf{K}_1$ are given as

$$\mathbf{K}_n = \sum_{\mathbf{k}\sigma\nu} \tau(\mathbf{k})\mathbf{v}_k^\nu \mathbf{v}_k^\nu \left(-\frac{\partial f(\varepsilon)}{\partial \varepsilon}(\mathbf{k}) \right) \left(\varepsilon_{\mathbf{k}}^\nu - \mu\right)^n, \tag{4}$$

where $\mathbf{k}$ is the wave vector, τ is quasiparticle lifetime, $\varepsilon_{\mathbf{k}}^\nu$ is the νth energy eigenvalue at $\mathbf{k}$, $\mathbf{v}_{\mathbf{k}}^\nu = (1/\hbar)(d\varepsilon_{\mathbf{k}}^\nu/d\mathbf{k})$ is the group velocity tensor, f is the Fermi distribution function, and μ is the chemical potential at T. We simply denote $(K_n)_{zz} = K_n$, $S_{zz} = S = (1/eT)(K_0/K_1)$, and $\rho_{zz} = \rho = e^{-2}K_0^{-1}$. We will approximate the quasiparticle lifetime as an (undetermined) constant in the present study, so that it cancels out in the Seebeck coefficient calculation, while not in the resistivity. Thus the absolute value of the power factor S^2/ρ is not determined and will be normalized by a certain value.

The calculated Seebeck coefficient as a function of the temperature is shown in Fig. 3. The results at $T = 300$ K give $-100\ \mu$V/K at $x = 0.025$, and $-77\ \mu$V/K at $x = 0.05$. The theoretical results are qualitatively in agreement with the experimental results, but quantitatively are about 20% smaller at $x = 0.025$ and $T = 300$ K.

In Fig. 4, we show the doping level dependence of the Seebeck coefficient and the normalized power factor (normalized by the maximum value) at $T = 300$ K. This

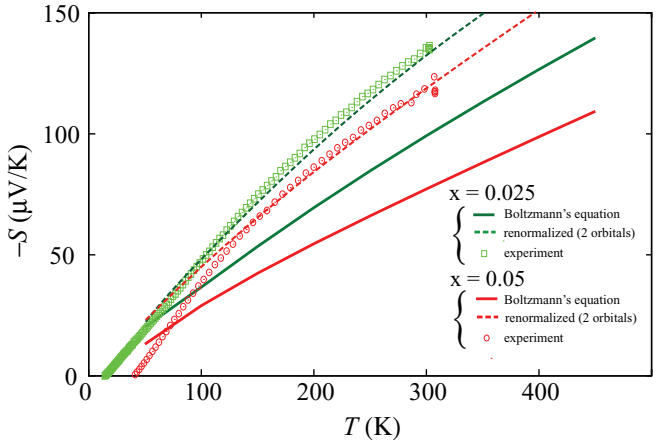

FIG. 3. (Color online) The calculated Seebeck coefficient for $x = 0.025$ and $x = 0.05$ using bare band structure (the solid lines) and renormalized band structure (the dashed lines) compared with the experimental result (green squares and red circles).

result shows that the Seebeck coefficient keeps relatively large values of about -50 μV/K even at a (hypothetically) large doping rate $x \simeq 0.5$, so that (assuming a constant quasiparticle lifetime) the power factor is roughly constant. This peculiar doping level dependence of the power factor is a consequence of the pudding-mold-type band.

Let us now focus more quantitatively on the discrepancy between the calculated results and the experiment. There may be several possibilities for the origin of this discrepancy: the constant lifetime approximation, or the bandwidth renormalization due to the electron correlation effects beyond GGA in the first-principles band calculation. As for the latter possibility, it has been known from the comparison between the band calculation and the angle-resolved photoemission studies that the bandwidth of the $3d$ electron materials can be reduced by as much as 60%, and taking this effect into account in the Seebeck coefficient calculation reproduces quantitatively the experimental results of Na_xCoO_2.[19,26] The Seebeck coefficient is underestimated also in other cases of $3d$ electron systems such as $SrTiO_3$,[18] due to the bandwidth renormalization effect, or the momentum/energy dependence of the quasiparticle lifetime.

In order to see the effect of the bandwidth renormalization in the present material, we consider electron correlation effects by applying the fluctuation exchange (FLEX) approximation,[27] which takes into account the effect of spin and charge fluctuations. In FLEX, bubble-and-ladder-type diagrams consisting of renormalized Green's functions are summed up to obtain the susceptibilities, which are used to calculate the self-energy self-consistently. The renormalized Green's functions are then determined self-consistently from the Dyson's equation. In the low-energy regime near the Fermi level, the quasiparticle dispersion $\omega_{\mathbf{k}}$ can be given by

$$\mathrm{Det}\left|\left(z^l_{\mathbf{k}}\omega_{\mathbf{k}} - \mu\right)\delta_{lm} - H^{lm}_{\mathbf{k}} - \mathrm{Re}\Sigma^R(\mathbf{k},\omega = 0)\right| = 0, \quad (5)$$

where l and m are orbital indices, z is the mass enhancement factor, Σ^R is the retarded self-energy, and H is the tight-binding Hamiltonian, respectively. We approximate the retarded self-energy $\Sigma^R(\mathbf{k},\omega = 0)$ as the self-energy at lowest Matsubara frequency $\Sigma(\mathbf{k},i\pi k_B T)$. The mass enhancement factor is obtained as

$$z_{\mathbf{k}} = 1 - \left.\frac{\partial\Sigma^R(k,\omega)}{\partial\omega}\right|_{\omega\to 0} \simeq 1 - \frac{\mathrm{Im}\Sigma(\mathbf{k},i\pi k_B T)}{\pi k_B T}, \quad (6)$$

where Σ is the self-energy at lowest Matsubara frequency. We take $32 \times 16 \times 32$ k-point meshes, 4096 Matsubara frequency, $T = 0.01$ eV, and an on-site interaction of $U = 2.5$ eV. The renormalized band structure at $x = 0.025$ and 0.05 is shown in Fig. 5. It can be seen that the bandwidth is monotonically reduced as the electrons are doped. The Seebeck coefficient

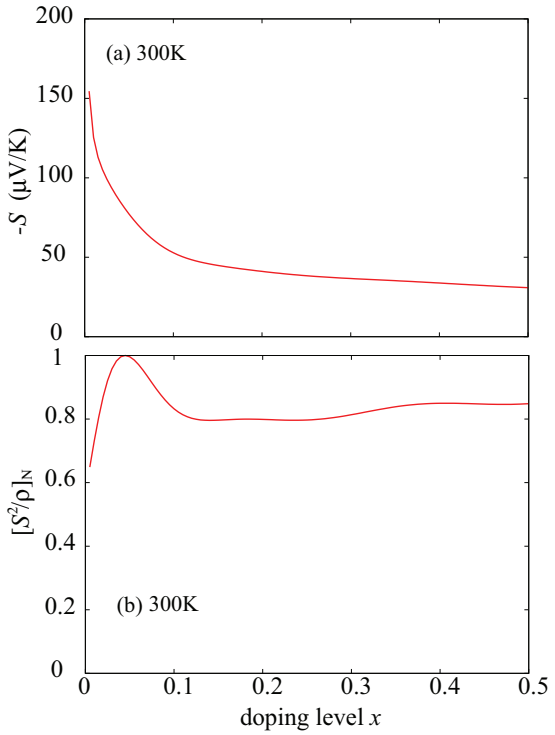

FIG. 4. (Color online) (a) The calculated Seebeck coefficient and (b) the normalized power factor at 300 K against the doping level x.

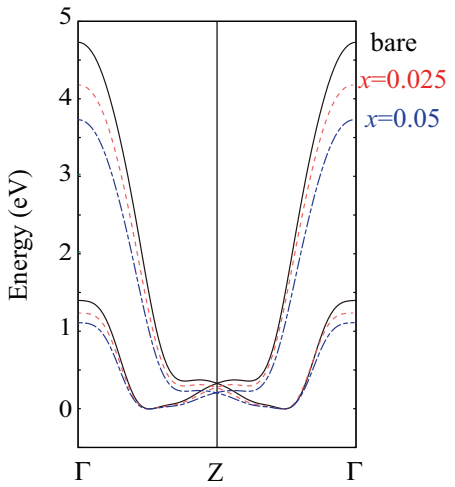

FIG. 5. (Color online) (a) The renormalized band structure at $x = 0.025$ (dashed lines) and $x = 0.05$ (dashed-dotted lines), and the bare band structure (solid line).

calculated by using the renormalized band structure is shown in Fig. 3 (dashed lines), which is now in very good agreement with the experimental results. The enhancement of the Seebeck coefficient from those obtained for the bare (unrenormalized) band is of course dependent on the value of the on-site repulsion U, but it is important to note that the agreement with the experimental results is obtained for a typical and realistic U value for a $3d$ orbital, which has been investigated theoretically in detail for the cuprate or iron-based superconductors. Although we have not studied other possibilities for the origin of the discrepancy between experiment and theory, the present analysis suggests that the bandwidth renormalization plays an important role as in other $3d$ thermoelectric materials such as Na_xCoO_2.

C. Origin of the pudding-mold-type band

As seen from our theoretical analysis, the large Seebeck coefficient in the electron-doped $FeAs_2$ is a consequence of the q1D pudding-mold-type band. In this section, we focus on the origin of this peculiar band structure. For simplicity, we first consider a unit cell that contains only one Fe site per unit cell. This corresponds to expanding (unfolding) the Brillouin zone. By taking this unit cell, we consider a simplified tight-binding model, where only the hoppings t_{1z} and t_{2z} along z direction, and t_{xyz} to the $(1/2,1/2,1/2)$ position, are considered [Fig. 6(a), see Fig. 6(b) for the correspondence with the actual lattice structure]. The hoppings in the x and y directions can be neglected for the band originating from the

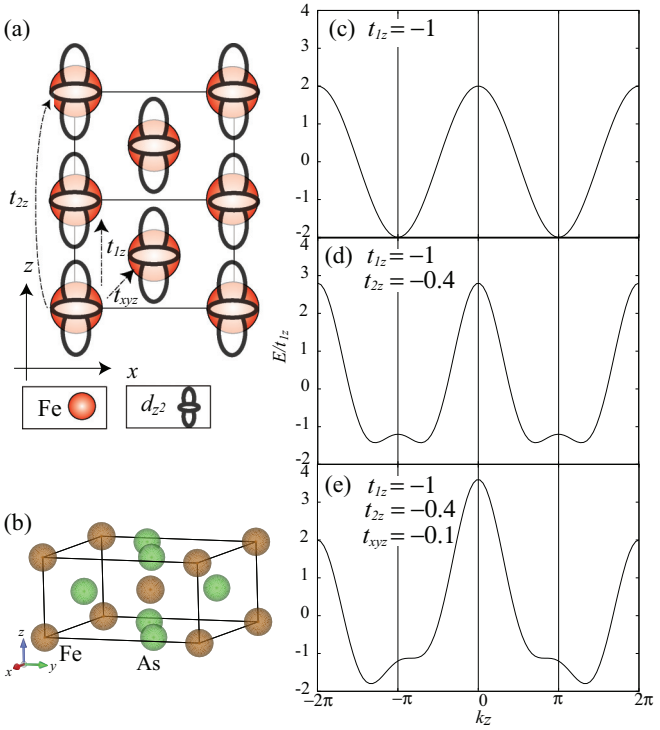

FIG. 6. (Color online) (a) A simplified tight-binding model of $FeAs_2$ and (b) crystal structure of $FeAs_2$. The band structure in the unfolded Brillouin zone is shown in the right panel with (c) $t_{1z}=-1$, (d) $t_{1z}=-1$ and $t_{2z}=-0.4$, and (e) $t_{1z}=-1$, $t_{2z}=-0.4$, and $t_{xyz}=-0.1$.

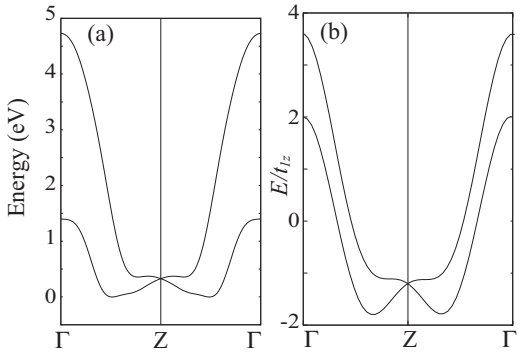

FIG. 7. (a) The two-orbital tight-binding model constructed from MLWFs and (b) the band structure of Fig. 6(e) shown in the folded Brillouin zone.

d_{z^2} orbital. In this model, the energy is given as

$$E(\mathbf{k}) = -2t_{1z}\cos(k_z) - 2t_{2z}\cos(2k_z) - 8t_{xyz}\cos(k_x/2)\cos(k_y/2)\cos(k_z/2). \quad (7)$$

When $k_z \simeq \pi$, the third term in the right-hand side vanishes due to $\cos(\pi/2)=0$ and the band dispersion loses k_x and k_y dependence. This is the explanation of the q1D nature of the band structure in the $k_z=\pi$ plane. We now focus on the band structure along the k_z direction. When we consider only t_{1z}, the band shape is free-electron-like at the bottom of the band [Fig. 6(c)]. Adding the distant hopping $t_{2z}=-0.4$, the shape of the band becomes flat near the band edge around $k_z=\pi$ (corresponding to the Z point), so that the q1D pudding-mold-type band is formed [Fig. 6(d)]. Furthermore, considering $t_{xyz}=-0.1$, the band becomes asymmetric with respect to $k_z=\pi$ [Fig. 6(e)].

To compare this simple band structure to a more realistic one, we construct, again exploiting the MLWFs, a two-orbital model that considers only the d_{z^2} orbital in the original unit cell that contains two Fe. Although this model does not perfectly reproduce the original band structure as in the six-orbital model presented above, it still captures the essential features. In this model, $t_{1z}=-0.62$ eV, $t_{2z}/t_{1z}=0.26$, $t_{xyz}/t_{1z}=0.28$, and the distant hoppings are also contained. The band structure of the two-orbital model is shown in Fig. 7(a) compared with the band structure of Fig. 6(c) refolded into the original Brillouin zone [Fig. 7(b)]. The band structure of the simplified model is roughly similar to that of the two-orbital model, especially near the band bottom, so that the essence of the origin of this peculiar band structure can be understood by the simplified model. To be precise, the magnitude of t_{2z} and t_{xyz} is different between the two models because the simplified model considers only three hoppings, while the more realistic two-orbital model takes into account the distant hoppings as well. The bottom line here is that the origin of the q1D pudding-mold-type band is the overlapping feature of the d_{z^2} orbitals, where a relatively large second-neighbor hopping is present.

IV. CONCLUSION

In the present work, we have studied the thermoelectric properties of the electron-doped $FeAs_2$. A large Seebeck

coefficient is observed despite the metallic behavior of the resistivity. First-principles band calculation reveals the presence of a q1D pudding-mold-type band just above the band gap, which mainly originates from the Fe $3d_{z^2}$ orbital. Using a tight-binding model that correctly reproduces this band structure, we have calculated the Seebeck coefficient. The results are close to the experimental observation, but quantitatively about 20% percent smaller. We also find that this discrepancy is greatly overcome when the bandwidth renormalization due to electron correlation effects beyond GGA is considered.

The q1D nature of the pudding-mold-type band comes from the combination of the d_{z^2} orbital and the lattice structure. Given the present study, we now have examples of materials that possess one-, two-, or three-dimensional flatbands that give rise to the large Seebeck coefficient in a metallic system. Therefore the present findings in the electron-doped $FeAs_2$ reinforce the general efficiency of peculiar band shapes with partially flat dispersion.

Another significant meaning for studying bands having quasi-1D nature is that we can clearly understand the origin of the pudding-mold shape. In the present case, the flat portion of the band originates from a destructive interference between $t_{1z}\cos(k_z)$ and $t_{2z}\cos(2k_z)$ terms (addition at wave vectors that give the opposite sign between the two terms), while the dispersive portion comes from a constructive interference between the two. Multiple electron hopping paths from one site to another can in general result in such destructive or constructive interferences depending on the wave number, and thus can result in a pudding-mold shape of the band. In this sense, geometrically frustrated lattice structures, as in Na_xCoO_2, are in general favorable, provided that the orbitals are not localized too much.

[1] For a general review on the theoretical aspects as well as experimental observations of thermopower, see G. D. Mahan, Solid State Phys. **51**, 81 (1997).

[2] I. Terasaki, Y. Sasago, and K. Uchinokura, Phys. Rev. B **56**, R12685 (1997).

[3] T. Caillat, M. Carle, P. Pierrat, H. Scherrer, and S. Scherrer, J. Phys. Chem. Solids **53**, 1121 (1992).

[4] H. Kuriyama, M. Nohara, T. Sasagawa, K. Takubo, T. Mizokawa, K. Kimura, and H. Takagi, *Proceedings of the 25th International Conference on Thermoelectrics* (IEEE, Piscataway, NJ, 2006).

[5] S. Shibasaki, W. Kobayashi, and I. Terasaki, Phys. Rev. B **74**, 235110 (2006).

[6] Y. Okamoto, S. Niitaka, M. Uchida, T. Waki, M. Takigawa, Y. Nakatsu, A. Sekiyama, S. Suga, R. Arita, and H. Takagi, Phys. Rev. Lett. **101**, 086404 (2008).

[7] S. Shibasaki, Y. Takahashi, and I. Terasaki, J. Phys.: Condens. Matter **21**, 115501 (2009).

[8] T. Okuda, K. Nakanishi, S. Miyasaka, and Y. Tokura, Phys. Rev. B **63**, 113104 (2001).

[9] H. Ohta, K. Sugiura, and K. Koumoto, Inorg. Chem. **47**, 8429 (2008).

[10] Y. Nishikubo, S. Nakano, K. Kudo, and M. Nohara, Appl. Phys. Lett. **100**, 252104 (2012).

[11] D. J. Singh, Phys. Rev. B **61**, 13397 (2000).

[12] K. Mori, H. Usui, H. Sakakibara, and K. Kuroki, AIP Adv. **2**, 042108 (2012).

[13] P. Wissgott, A. Toschi, H. Usui, K. Kuroki, and K. Held, Phys. Rev. B **82**, 201106 (2010).

[14] G. B. Wilson-Short, D. J. Singh, M. Fornari, and M. Suewattana, Phys. Rev. B **75**, 035121 (2007).

[15] W. Koshibae and S. Maekawa, Phys. Rev. Lett. **87**, 236603 (2001); W. Koshibae, K. Tsutsui, and S. Maekawa, Phys. Rev. B **62**, 6869 (2000).

[16] R. Arita, K. Kuroki, K. Held, A. V. Lukoyanov, S. Skornyakov, and V. I. Anisimov, Phys. Rev. B **78**, 115121 (2008).

[17] H. Usui, R. Arita, and K. Kuroki, J. Phys.: Condens. Matter **21**, 064223 (2009).

[18] H. Usui, S. Shibata, and K. Kuroki, Phys. Rev. B **81**, 205121 (2010).

[19] K. Kuroki and R. Arita, J. Phys. Soc. Jpn. **76**, 083707 (2007).

[20] P. Sun, N. Oeschler, S. Johnsen, B. B. Iversen, and F. Steglich, Appl. Phys. Express **2**, 091102 (2009).

[21] A. Bentien, S. Johnsen, G. K. H. Madsen, B. B. Iversen, and F. Steglich, Europhys. Lett. **80**, 17008 (2007).

[22] J. M. Tomczak, K. Haule, T. Miyake, A. Georges, and G. Kotliar, Phys. Rev. B **82**, 085104 (2010).

[23] P. Blaha, K. Schwarz, G. Madsen, D. Kvasnicka, and J. Luitz, *WIEN2k, An Augmented Plane Wave + Local Orbitals Program for Calculating Crystal Properties* (Karlheinz Schwarz, Techn. Universität Wien, Austria, 2001). Here we take $RK_{\max} = 7$, 512 k points, and adopt the exchange correlation functional introduced by J. P. Perdew, K. Burke, and M. Ernzerhof, Phys. Rev. Lett. **77**, 3865 (1996).

[24] H. D. Lutz, M. Jung, and G. Wäschenbach, Z. Anorg. Allg. Chem. **554**, 87 (1987).

[25] N. Marzari and D. Vanderbilt, Phys. Rev. B **56**, 12847 (1997); I. Souza, N. Marzari, and D. Vanderbilt, *ibid.* **65**, 035109 (2001); The Wannier functions are generated by the code developed by A. A. Mostofi, J. R. Yates, N. Marzari, I. Souza, and D. Vanderbilt, http://www.wannier.org/.

[26] The reduction of the bandwidth results in a decrease in the group velocity and an enhancement of the DOS (roughly proportional to the inverse of the velocity). The reduction of the group velocity cancels out between the denominator and the numerator in the Seebeck effect, so that the increase of the density of states gives a larger Seebeck coefficient.

[27] N. E. Bickers, D. J. Scalapino, and S. R. White, Phys. Rev. Lett. **62**, 961 (1989).